Sixth International Conference on Durability of Concrete Structures **Paper Number PSE11**
18 - 20 July 2018
University of Leeds, Leeds, West Yorkshire, LS2 9JT, United Kingdom

Freeze-thaw resistance of concrete: Insight from microstructural properties

S. Adu-Amankwah and L. Black
School of Civil Engineering, University of Leeds, UK

M. Zajac, J. Skocek and M. Ben Haha
Heidelberg Technology Center GmbH, Leimen, Germany

ABSTRACT

Composite cements offer low carbon alternatives to conventional CEM I. These binders also generally tend to perform better than CEM I in aggressive chemical environments. However, their freeze-thaw resistance, evident through surface scaling and internal damage is usually impaired. Postulated theories on freeze-thaw induced damage do not fully explain the origin of this weakness in composite cement concretes.
This paper systematically presents the phase assemblage changes associated with the freeze-thaw of concrete specimen made from composite cements with and without limestone. The freeze-thaw test was performed on concrete according to CIF method based on CEN/TR 15177 and the corresponding cement pastes characterized by X-ray powder diffraction (XRD) and thermogravimetric analysis (TGA). In all investigated composite cements, portlandite was already depleted after the 7d capillary suction. The implications of this and other modified assemblages during the conditioning and the freeze-thaw test are consequently discussed.

Keywords: Limestone ternary cement, durability, freeze-thaw, microstructure.

1.0 INTRODUCTION

Composite cements, which are low carbon alternatives to CEM I face some challenges. They are often characterized by slow rates of hydration of the supplementary cementitious materials (SCM) and hence a slower evolution of the microstructure compared to CEM I (Atiş, 2003; Bouikni *et al.*, 2009). In the long term however, progressive hydration of the SCM offsets this, leading to improved mechanical properties and durability (Ghirci *et al.*, 2007). However, reference methodologies for durability testing are not designed to take the slower kinetics into account in their assessment. Consequently, reduced durability particularly following accelerated tests such as carbonation (Borges *et al.*, 2010) and freeze-thaw (Deja, 2003; Stark and Ludwig, 1997) have been reported.

In the reference ASTM C666, freeze-thaw testing commences after 14 d curing whereas in CEN/TR 15177 testing starts after 28 d. The test protocol in the latter however comprises of 7 d moist curing followed by 21 d conditioning at 65 % RH at 20 °C. At 28 d, the specimens are saturated by capillarity action for a further 7 d before commencing the freezing and thawing cycles (PDCEN/TR15177, 2006; Setzer *et al.*, 2004). A shortening of the moist-curing duration has been shown to retard the progress of further hydration (Ramezanianpour and Malhotra, 1995) while the conditioning regime at 65 % RH also favours carbonation (Ho *et al.*, 1989). Additionally, capillary suction in demineralized water potentially accelerates leaching (Carde and François, 1999; Rozière and Loukili, 2011) and hence could modify the microstructure even before being subjected to freeze-thaw. Clarifying the effects induced by this testing methodology is vital for analyzing the strengths and weakness of different cement formulations during freeze-thaw testing.

The glue-spall mechanism has been espoused to explain surface scaling due to freeze-thaw (Valenza Ii and Scherer, 2007). By this hypothesis, scaling arises from cracks propagating from the frozen water on the surface and into the concrete. The validity of this mechanism however hinges on moderate salt concentrations in the test solution. Alternative hypotheses are the hydraulic pressure and the microscopic ice-lens theories (Setzer, 2001). These attribute deterioration to ice-growth in critically saturated concrete pores.
Potential methodological flaws in addition to divergent controlling hypothesis are obvious. This paper therefore systematically investigates modifications in the phase assemblages at key stages of the conditioning and freeze-thaw test. The impact of these changes are further discussed.

2.0 MATERIALS AND METHODS

2.1 Materials

Three types of cement: 50 % CEM I 52.5 R + 50 % GGBS, 50 % CEM I 52.5 R + 40 % GGBS + 10 % limestone and 50% CEM I 52.5R+30% GGBS + 20% limestone herein referred to as CS, CS-L and CS-2L respectively were studied. These were produced by blending the SCM with commercial CEM I 52.5 R. Anhydrite was used to adjust the sulfate content of the composite cements to match that of a reference CEM I mix (Adu-Amankwah *et al.*, 2017b). The constituent compositions, as determined by XRF, are detailed in Table 1.

The concrete mix design was based on the yield method, taking into account the specific gravities of all constituent materials. The w/c ratio was maintained at 0.5 after allowing for absorption by the aggregates. The following predefined values were kept constant in the mix designs: cement content of 320.3kg/m^3, 2.5% total air and 0.54 fine to coarse aggregate ratio. The coarse aggregates were a blend of 10 and 20 mm quartzite, the ratio optimized for workability and maintained for all mixes. No air entrainment admixtures were used. The resulting proportions per cubic metre of concrete are listed in Table 2.

2.2 Sample preparation

Concrete samples were prepared according to EN 12390:2 (BSI, 2009). The mixing procedure for concrete involved dry mixing of aggregates and cement in a 60-litre drum mixer for homogeneity. After adding the water, mixing continued for 30 seconds and materials adhering to the sides and bottom of the mixing pan were scraped. The concrete was mixed for further 60 seconds and testing for fresh properties commenced 10 minutes after mixing. Cubes for compressive strength and carbonation testing were 100 mm, while 150 mm cubes were used for freeze-thaw testing. Specimens were kept in the mould for 24 hours before de-moulding, after which samples were transferred to a water bath at 20 ◦C to 7 days.

2.3 Methods

The freeze-thaw testing was performed by the CIF method according to PD CEN/TR 15177: 2006 i.e. in deionized water. A complete freezing and thawing cycle took 24 hours as opposed to the 12 hours prescribed in the standard. The modification was imposed by the freeze-thaw chamber used (Adu-Amankwah *et al.*, 2017a).

The scaled mass was collected at regular intervals after 3-minutes cleaning in a sonic bath. These were then dried at 40 ◦C to constant mass in a glovebox. The deviation from the prescribed 110 ± 10 °C drying temperature was to preserve all phase assemblages in the specimen, particularly ettringite and carboaluminate. Internal structural damage was determined based on regular measurement of the transit time using a Proceq Pundit Lab+ ultrasonic pulse.

The microstructure and phase assemblage were characterized by thermal analysis and XRD on cement pastes. These were prepared according to CIF test method, replicating the test surface during the freeze-thaw. After the 7d moist curing, the paste samples were crushed into 1 – 2 mm thick powders. These were then conditioned at 65 % RH at 20 ◦C for 21 d before saturating for a further 7 d and then freeze-thawed.

Thermogravimetric analysis (TGA) was performed under nitrogen on 16-18mg of additionally ground paste samples, using a Stanton 780 Series Analyzer. The heating range was 20-1000°C at a rate of 20°C/minute. XRD data were acquired on a Bruker D2 Phaser using a Cu anode operating at 30kV and 10mA, over a range of 5-70 °2θ. The step size was 0.0344 °2θ, using the Lynxeye detector.

Table 1. Oxide composition of raw materials (%wt.)

Composition	SiO_2	Al_2O_3	MgO	CaO	K_2O	Na_2O	SO_3	Blain (m^2/kg)
CEM I 52.5 R[C]	20.37	5.56	1.65	62.10	0.65	0.49	3.54	593
Slag [S]	34.87	11.62	5.82	41.82	0.47	0.01	3.13	454
Limestone [L]	2.00	0.08	0.64	53.13	0.10	-	0.07	328
Anhydrite	2.94	0.60	1.45	38.32	0.16	-	52.24	472

Table 2. Concrete mix proportions, kg/m^3 (composite cements designed so as to contain 3% sulfate content)

Mix ID	CEMI	Slag	Limestone	Anhydrite	Water	Aggregates		
						Fine	10mm	20mm
CS	162.3	150.8	-	7.2	160.2	648.8	236.6	946.4
CS-L	163.9	121.8	27.4	7.2	160.2	648.1	236.4	945.5
CS-2L	163.9	91.3	57.8	7.2	160.2	647.4	236.1	944.5

3.0 RESULTS

3.1 Overview of freeze-thaw as a function of cement composition

Representative photographs of concrete mixes CS and CS-2L at the end of the 56th freeze-thaw cycle are shown in Fig 1. Significant loss of surface matter can be seen. The limestone containing composite cements however exhibited higher scaling.

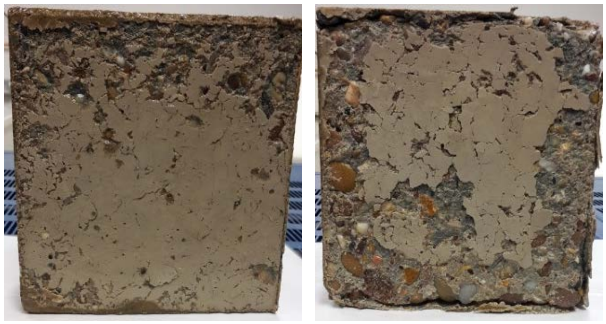

Fig. 1. Representative photographs after 56 freeze-thaw cycles (right mix CS, left mix CS-2L).

The internal damage and mass of scaled matter were measured over the duration of the test and the results shown in Fig 2. Significant loss of the relative dynamic modulus of elasticity (RDME) was apparent after 7 freeze-thaw cycles. However, differences performance for the different cement compositions became clearer after this. The RDME for mix CS-2L was already lower than the 80 % failure criterion by the 15th cycle while this threshold was reached by CS-L and CS at the 26th and 35th cycles respectively. At the end of the 56th cycle, the RDME loss was 50 - 60% in the ternary blends whereas that of mix CS was ~ 35 %. Meanwhile, scaling was relatively small until the 35th cycle (< 50 m^2/g). Significantly higher scaled matter was measured in all mixes from the 35th cycle onwards, being highest in CS-2L.

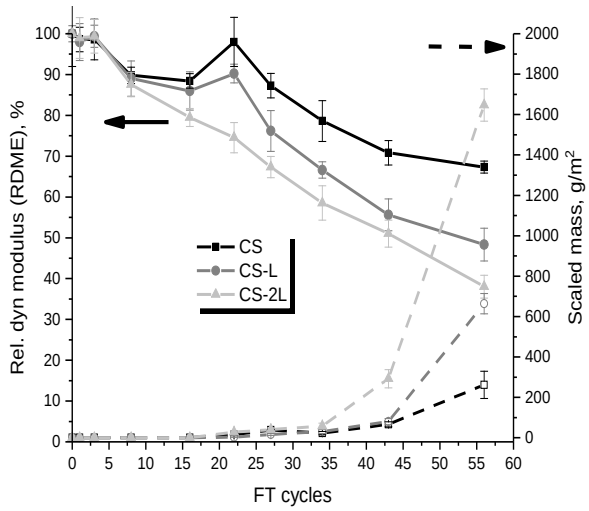

Fig. 2. Effect of cement composition on the freeze-thaw resistance measured by the CIF method.

3.2 Microstructural changes arising from freeze-thaw

The scaling and internal damage measurements indicated CS and CS-2L as the best and worse mixes respectively. Consequently, the microstructural investigations focused on these two mixes. The derivatives of the TGA curves were calculated and used for the analysis in order to reveal modifications associated with the individual assemblages. XRD meanwhile focused on the ettringite, carboaluminate and portlandite contents, which are the main crystalline hydrated assemblages. Hence data are shown only over the range 8 – 18.5 °2Θ.

Fig 3 shows the DTG plots of the two mixes at key stages during the conditioning and also the freeze-thaw test. The data is presented up to the 25th FT cycle because some of the cement pastes showed significant disintegration at this point.

A reduction in the endothermal peak associated with the decomposition of C-S-H and ettringite can be seen in both mixes between 7 and 28 days where the samples were exposed to 65% RH and 20°C. Meanwhile a reduction in the portlandite content over the same period was also observed. A notable increase in the calcite content resulted from the conditioning. The XRD patterns in Fig 4 corroborated the DTG trace, indicating reductions in the ettringite and portlandite peak intensities with concomitant increase in the calcium carbonate content resulting from the 21 d conditioning. The low DTG decomposition temperature is suggestive of an initially amorphous calcium carbonate.

The 7 d saturation of the samples in deionized water was also accompanied by further modifications in the aforementioned assemblages. A significant increase in the C-S-H and ettringite peak is noticed in Fig 3 for both mixes. Fig 4 however indicates more ettringite following the saturation of the samples which could partly explain the DTG observations. A more significant effect of saturation was in the loss of portlandite, as indicated by the DTG and XRD in Fig 3 and 4 respectively. More intense XRD peaks due to C-S-H and ettringite as well as calcite could partly explain the loss of portlandite. Analysis of the test solution (not reported here) however confirmed leaching of calcium. In addition, the amorphous calcium carbonate, present at early stages as mentioned above was replaced over time with a more crystalline phase, evidenced by a shift towards a higher temperature (Perić *et al.*, 1996). The mono and hemi-carboaluminate balance was not distinctively affected by the preceding conditioning and saturation. Consistently, hemi-carboaluminate was predominant in mix CS while mono-carboaluminate was present in CS-2L (Fig 4).

At the point of noticeable cement paste disintegration, the C-S-H and ettringite peaks from the DTG were more pronounced, while portlandite was depleted.

The change in calcite content between the saturation and disintegration of the samples was insignificant. Indeed, a further increase in carbonation was not expected at about 100 % RH (Ho *et al.*, 1989).

4.0 DISCUSSION

These results highlight the importance of the microstructure at the start and during the conditioning and freeze-thaw test. Potential implications of the said changes on the macroscale observations are subsequently discussed and conclusions drawn.

The fact that the composite cements contained less portlandite increased susceptibility to carbonation. Carbonation of the C-S-H, ettringite and portlandite (Fig 3 and 4) also has implications on the pore structure (Goñi *et al.*, 2002; Morandeau *et al.*, 2015) and consequently the mechanical properties. In the composite cements, capillary porosity increases upon carbonation, further raising the volume of the test solution, which may be admissible during the saturation and also the freeze-thaw cycles.

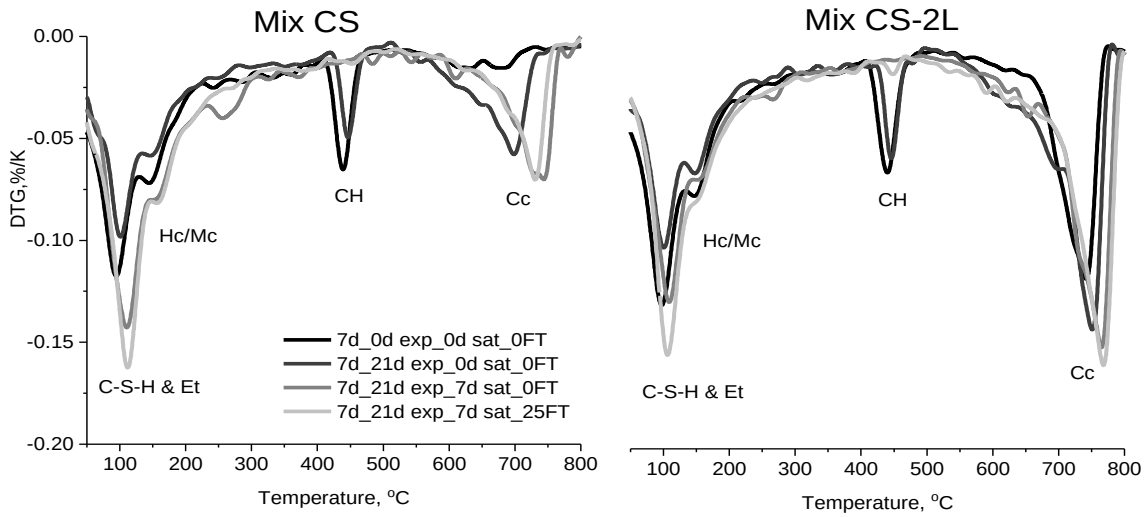

Fig.3. Effect of the cement composition on the microstructure as a function of conditioning before and during freeze-thaw, analyzed by TG

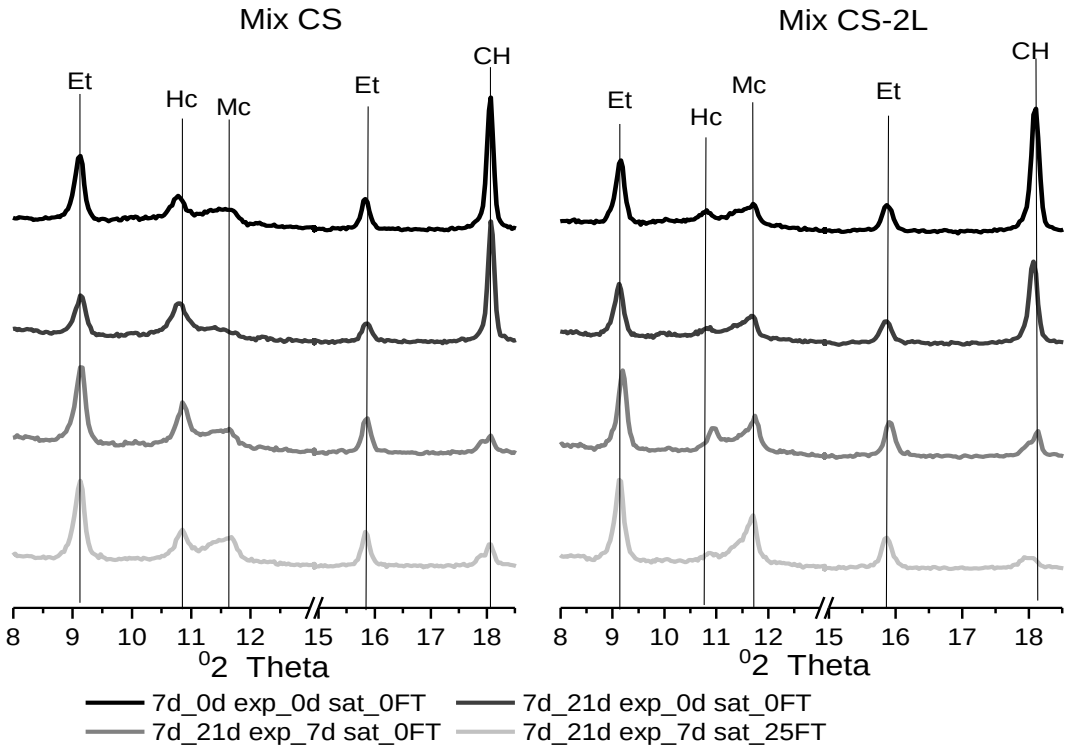

Fig.4. Effect of the cement composition on the microstructure as a function of conditioning before and during freeze-thaw, analyzed by XRD

Carbonation of portlandite and ettringite could influence porosity similarly. The fact that ettringite occupies a significantly higher volume than to calcite implies an increase in the capillary pore volume after carbonation. This would increase the volume of pores which could become saturated once the samples were in contact with water.

Saturation of the pre-dried (and carbonated) samples was found to result in depletion of portlandite in the investigated samples. The reformation of ettringite (Fig 3 and 4) was noted as already discussed. However, if a closed system is assumed, the portlandite consumed in reforming ettringite should be no more than what that which was originally present at the start of the conditioning process. Portlandite uptake to form new hydrates during the saturation period cannot be discounted either. However, concurrent reaction of the clinker and the newly formed hydrates is plausible. Hence, renewed hydration during the saturation may not also fully explain the significant loss of portlandite. Leaching of calcium is the most likely explanation for the depleted portlandite, and leaching from the C-S-H cannot be discounted. Studies reported elsewhere (Carde and François, 1999) identified macro-porosity as a result of calcium leaching from portlandite as opposed to micro-pores resulting from the C-S-H. The increased macro-porosity was more detrimental to the mechanical properties. Moreover, being inherently resistant to deformation compared to the C-S-H (Nguyen *et al.*, 2013), portlandite potentially provides restraints in a manner analogous to defects within a continuous matrix. Consequently the depletion could further weaken the hydrated cement.

Lower freeze-thaw resistance in the ternary blends and with increasing limestone dosage seems to be associated with the phase distributions, porosity and the effect of the sample preparation protocol as already discussed. At a given CEM I replacement, the portlandite content decreased as the limestone content while the capillary pore volume also increased (Adu-Amankwah *et al.*, 2017b). The combined effects could explain the reduced freeze-thaw resistance in the composite cements.

The presence of limestone is known to accelerate the hydration of clinker and slag as well as refine the pore structure (Adu-Amankwah *et al.*, 2017b; Berodier and Scrivener, 2015). Whereas the accelerated slag hydration refines gel pores, the capillary porosity tends to increase. Beside kinetics, the cements from which the concretes were made also differed in their capillary porosities, while the gel pores were similar at 28 d (Adu-Amankwah *et al.*, 2017b). The capillary pores have been shown to provide reservoirs for drawn water as well as acting as colonies for ice growth as opposed to the gel pores.

5.0 CONCLUSIONS

The freeze-thaw resistance of concrete formulated from composite cements and the corresponding microstructures have been studied at 0.5 w/c ratio without air entraining admixtures. The ternary cement concretes had lower resistance compared to the binary blend. Characterization of the microstructures identified the loss of portlandite to carbonation and leaching as the dominant changes arising from the test. Both could increase capillary porosity and consequently the number of freezing sites and thus leading to a reduced resistance to freeze-thaw. The observations highlight potential pitfalls for low clinker cements. The conclusions include a requirement to modify the experimental methodology which promotes a weakened microstructure prior to the test. Alternatively, allowing sufficient microstructure development of the matrix before commencing the test could overcome some of the identified methodological deficiencies in low clinker composite cements.

References

Adu-Amankwah, S., Zajac, M., Skocek, J., Ben Haha, M., Black, L., 2017a. Relationship between cement composition and the freeze–thaw resistance of concretes. Advances in Cement Research: 1-11. DOI:10.1680/jadcr.17.00138

Adu-Amankwah, S., Zajac, M., Stabler, C., Lothenbach, B., Black, L., 2017b. Influence of limestone on the hydration of ternary slag cements. Cement and Concrete Research, 100: 96-109. DOI:https://doi.org/10.1016/j.cemconres.2017.05.013

Atiş, C.D., 2003. Accelerated carbonation and testing of concrete made with fly ash. Construction and Building Materials, 17(3): 147-152. DOI:10.1016/s0950-0618(02)00116-2

Berodier, E., Scrivener, K., 2015. Evolution of pore structure in blended systems. Cement and Concrete Research, 73: 25-35. DOI:http://dx.doi.org/10.1016/j.cemconres.2015.02.025

Borges, P.H.R., Costa, J.O., Milestone, N.B., Lynsdale, C.J., Streatfield, R.E., 2010. Carbonation of CH and C–S–H in composite cement pastes containing high amounts of BFS. Cement and Concrete Research, 40(2): 284-292. DOI:http://dx.doi.org/10.1016/j.cemconres.2009.10.020

Bouikni, A., Swamy, R.N., Bali, A., 2009. Durability properties of concrete containing 50% and 65% slag. Construction and Building Materials, 23(8): 2836-2845. DOI:https://doi.org/10.1016/j.conbuildmat.2009.02.040

BSI, 2009. BS EN 12390-2,"Testing hardened concrete-Part 2: Making and curing specimens for strength tests", Brussels, Belgium: European Committee for Standardization.

Carde, C., François, R., 1999. Modelling the loss of strength and porosity increase due to the leaching of cement pastes. Cement and Concrete Composites, 21(3): 181-188. DOI:https://doi.org/10.1016/S0958-9465(98)00046-8

Deja, J., 2003. Freezing and de-icing salt resistance of blast furnace slag concretes. Cement and Concrete Composites, 25(3): 357-361. DOI:http://dx.doi.org/10.1016/S0958-9465(02)00052-5

Ghirci, M., Kenai, S., Said-Mansour, M., 2007. Mechanical properties and durability of mortar and concrete containing natural pozzolana and limestone blended cements. Cement and Concrete Composites, 29(7): 542-549.

Goñi, S., Gaztañaga, M., Guerrero, A., 2002. Role of Cement Type on Carbonation Attack. Journal of Materials Research, 17(7): 1834-1842. DOI: doi:10.1557/JMR.2002.0271

Ho, D.W.S., Cui, Q.Y., Ritchie, D.J., 1989. The influence of humidity and curing time on the quality of concrete. Cement and Concrete Research, 19(3): 457-464. DOI:http://dx.doi.org/10.1016/0008-8846(89)90034-3

Morandeau, A., Thiéry, M., Dangla, P., 2015. Impact of accelerated carbonation on OPC cement paste blended with fly ash. Cement and Concrete Research, 67: 226-236. DOI:http://dx.doi.org/10.1016/j.cemconres.2014.10.003

Nguyen, D.-T., Alizadeh, R., Beaudoin, J.J., Raki, L., 2013. Microindentation creep of secondary hydrated cement phases and C–S–H. Materials and Structures, 46(9): 1519-1525. DOI:10.1617/s11527-012-9993-0

PDCEN/TR15177, 2006. Testing the freeze-thaw resistance of concrete-Internal structural damage.

Perić, J., Vučak, M., Krstulović, R., Brečević, L., Kralj, D., 1996. Phase transformation of calcium carbonate polymorphs. Thermochimica Acta, 277: 175-186. DOI:https://doi.org/10.1016/0040-6031(95)02748-3

Ramezanianpour, A.A., Malhotra, V.M., 1995. Effect of curing on the compressive strength, resistance to chloride-ion penetration and porosity of concretes incorporating slag, fly ash or silica fume. Cement and Concrete Composites, 17(2): 125-133. DOI:10.1016/0958-9465(95)00005-w

Rozière, E., Loukili, A., 2011. Performance-based assessment of concrete resistance to leaching. Cement and Concrete Composites, 33(4): 451-456. DOI:https://doi.org/10.1016/j.cemconcomp.2011.02.002

Setzer, M.J., 2001. Micro-Ice-Lens Formation in Porous Solid. Journal of Colloid and Interface Science, 243(1): 193-201. DOI:https://doi.org/10.1006/jcis.2001.7828

Setzer, M.J. *et al.*, 2004. Test methods for frost resistance of concrete: CIF Test: Capillary suction, Internal damage and freeze thaw test - Referennce method and alternative methods A and B. Materials and Structures, 37: 743 - 753.

Stark, J., Ludwig, H.M., 1997. Freeze-deicing salt resistance of concretes containing cement rich in slag. In: Setzer, M.J., Auberg, R. (Eds.), Frost Resistance of Concrete. Proceedings of the International RILEM Workshop. E & FN SPON, University of Essen, pp. 123-138.

Valenza Ii, J.J., Scherer, G.W., 2007. A review of salt scaling: II. Mechanisms. Cement and Concrete Research, 37(7): 1022-1034. DOI:http://dx.doi.org/10.1016/j.cemconres.2007.03.003